

Uncertainty Quantification of the Pion-Nucleon Low-Energy Coupling Constants up to Fourth Order in Chiral Perturbation Theory

K. A. Wendt* and A. Ekström

*Department of Physics and Astronomy, University of Tennessee, Knoxville, Tennessee 37996, USA and
Physics Division, Oak Ridge National Laboratory, Oak Ridge, Tennessee 37831, USA*

B. D. Carlsson

Department of Fundamental Physics, Chalmers University of Technology, SE-412 96 Göteborg, Sweden

(Dated: 7:22pm Saturday 13th October, 2018)

We extract the statistical uncertainties for the pion-nucleon (πN) low energy constants (LECs) up to fourth order $\mathcal{O}(Q^4)$ in the chiral expansion of the nuclear effective Lagrangian. The LECs are optimized with respect to experimental scattering data. For comparison, we also present an uncertainty quantification that is based solely on πN scattering phase shifts. Statistical errors on the LECs are critical in order to estimate the subsequent uncertainties in *ab initio* modeling of light and medium mass nuclei which exploit chiral effective field theory. As an example of the this, we present the first complete predictions with uncertainty quantification of peripheral phase shifts of elastic proton-neutron scattering.

PACS numbers: 21.30.-x,13.75.Gx,13.75.Cs,02.60.Pn

Introduction.— Chiral effective field theory (χ EFT) for nuclear physics provides a theoretical framework for a common description of various nuclear processes through the systematic generation of two- three- and many- body interactions and currents. Undoubtedly, it has allowed advances in *ab initio* structure calculations of light [1] and medium mass [2–4] atomic nuclei. The quantitative predictions of χ EFT depend on the numerical values of a set of low-energy constants (LECs), which have become a limiting factor in medium mass nuclei where current sets of LECs fail to simultaneously predict binding, spectra, and radii. It is therefore relevant to constrain these LECs such that all predictions within the realm of applicability of χ EFT can be quantified together with statistical uncertainties. This is important for advancing modern many-body calculations into regions of the nuclear chart and the physical processes where experimental data for verification is limited, such as neutrino-less double beta decay or structure and reactions near the neutron drip line. We present results that constrain the πN -sector of χ EFT, with accompanying confidence intervals (CI), up to fourth order in the expansion of the effective Lagrangian. At this order, the sub-leading long range three-nucleon interaction enters, and will thus be fully constrained by the results presented here. Further, many operator currents, such as the axial-vector current, depend on only πN LECs and three nucleon contact LECs. Therefore careful uncertainty quantification of the πN LECs is also critical for comparing processes driven by these currents to experimental cross sections and decay measurements.

The χ EFT interaction Lagrangian \mathcal{L}_{eff} for atomic nuclei can be separated into two terms $\mathcal{L}_{\text{eff}} = \mathcal{L}_{NN} + \mathcal{L}_{\pi N}$,

and the two different contributions each depend explicitly on a distinctive set of LECs. The first term parametrizes the short-ranged contact-interactions and the second term describes the long-ranged and pion-mediated part of the two- and three-nucleon interaction. While the NN -contact sector must be constrained using nucleon-nucleon data, the LECs in $\mathcal{L}_{\pi N}$ can be determined from experimental πN scattering-data, completely separately from the NN terms. This is one example of how χ EFT can link separate physical processes that are relevant for the description of atomic nuclei. Previous constraints for the πN LECs have been determined from peripheral NN scattering phase shifts [5, 6] or πN elastic scattering phase shifts [7–9]. Indeed, these efforts have produced various sets of LECs that closely reproduce the respective phase shift analyses (either NN [10, 11] or πN [12–15]); however, the lack of reliable uncertainties on the input phase shifts prevents meaningful uncertainty quantification of the πN LECs. It should be noted that available scattering phase shifts are not experientially measured data, but the result of a partial-wave analysis of measured data. In contrast with previous determinations of the πN LECs, the analysis presented here is grounded in experimental scattering data. This allows us to estimate meaningful statistical uncertainties. For the first time we can therefore explore the consistency of χ EFT by predicting CIs for the peripheral NN phase shifts determined by πN -data.

Optimization.— We seek a set of πN LECs \mathbf{c}_* that min-

* kwendt2@utk.edu

TABLE I: Numerical values of the πN LECs that result from the optimization with respect to experimental observables. The resulting values are grouped from left to right in the order they appear in the Lagrangian.

| $\mathcal{O}(Q^1)$ LECs [GeV $^{-1}$] | $\mathcal{O}(Q^2)$ LECs [GeV $^{-2}$] | $\mathcal{O}(Q^3)$ LECs [GeV $^{-3}$] |
|---|---|---|
| c_1 -1.40 ± 0.12 | $\bar{d}_1 + \bar{d}_2$ $+5.80 \pm 0.14$ | \bar{e}_{14} $+1.53 \pm 0.31$ |
| c_2 $+1.71 \pm 0.33$ | \bar{d}_3 -5.66 ± 0.08 | \bar{e}_{15} -11.91 ± 0.87 |
| c_3 -4.56 ± 0.11 | \bar{d}_5 $+0.03 \pm 0.06$ | \bar{e}_{16} $+11.43 \pm 1.23$ |
| c_4 $+3.72 \pm 0.27$ | $\bar{d}_{14} - \bar{d}_{15}$ -11.50 ± 0.12 | \bar{e}_{17} $+0.73 \pm 0.51$ |
| | | \bar{e}_{18} $+0.57 \pm 1.36$ |

imize the least-squares objective function [16]:

$$\chi_{\text{red}}^2(\mathbf{c}, \mathbf{N}) = \frac{1}{n_{df}} \left(\sum_i R_i(\mathbf{c}, \mathbf{N})^2 + \sum_j r_j(\mathbf{N})^2 \right) \quad (1)$$

$$R_i(\mathbf{c}, \mathbf{N}) = \frac{N_{j_i} O_i^{\chi\text{EFT}}(\mathbf{c}) - O_i^{\text{Exp.}}}{\Delta_i^{\text{Exp.}}} \quad (2)$$

$$r_j(\mathbf{N}) = \frac{N_j - 1}{\Delta_j} \quad (3)$$

where $O_i^{\chi\text{EFT}}(\mathbf{c})$ denotes the value of the scattering observable computed from χEFT , while $O_{j_i}^{\text{Exp.}}$ and $\Delta_{j_i}^{\text{Exp.}}$ denotes the experimentally measured value and uncertainty, respectively, for the corresponding observable. \mathbf{c} is a vector of LECs spanning all included c_i , d_i , and e_i LECs. \mathbf{N} is a vector of normalization coefficients N_j , where all points from a single experimental angular distribution share the same N_j ; Δ_j encodes uncertainty of the experimental systematics for N_j . The number of degrees of freedom is given by $n_{df} = (n_d + n_N - n_{NF}) - (n_{\text{lecs}} + n_N)$, where n_d is the number of data included in the fit, n_{lecs} is the number of LECs being fit, and n_N is the number of unknown normalization coefficients and n_{NF} is the number of floated coefficients (contribute no residual term in r_j as $\delta_j = \infty$). For a given experiment j , the included data points run over a series of scattering angles at a fixed lab frame momentum Q_{Lab} .

For our fitting dataset, we adopt the database from the most recent πN partial wave analysis [14], referred to as WI08. By construction, χEFT is a low-energy theory, therefore we exclude data with lab-frame momentum $Q_{\text{Lab}} > 160$ MeV. This leaves us with an experimental database consisting of differential scattering cross-sections and polarization cross sections from $\pi^\pm + p \rightarrow \pi^\pm + p$ and $\pi^- + p \rightarrow \pi^0 + n$ processes. In total, there are $n_d = 1246$ data points, consisting of 1194 differential unpolarized cross-sections and 52 differential singly-polarized cross-sections. There are $n_N = 110$ normalization coefficients, with $n_{NF} = 9$ floated coefficients. There are other measurable observables, such as the spin rotation parameters, but experimental data only exists for momentum well beyond the range of validity of the EFT. The cutoff in lab frame momentum (160 MeV) was

chosen such that increasing or decreasing the cutoff would lead to a larger minimum value of $\chi_{\text{red}}^2(\mathbf{c}, \mathbf{N})$, maximizing amount of included data while avoiding fitting past the radius of convergence of the EFT.

For the calculated observables, we use the strong amplitudes presented in Ref. [9] (Refs. [8, 17–19] give a more complete presentation of the πN scattering amplitudes, but use a different power counting scheme for relativistic corrections.) For the strong amplitude, we adopt their conventions for fixing \bar{d}_{18} , absorbing $\bar{e}_{19,20,21,22,35,36,37,38, \bar{l}_3}$ into $c_{1,2,3,4}$. We also work with exact isospin symmetry and use an averaged pion mass ($m_\pi = (m_{\pi^0} + 2m_{\pi^\pm})/3$). We adopt the electromagnetic treatment that is used in the WI08 partial wave analysis, which is described in detail in Refs. [20–23]. For the electromagnetic corrections, we explicitly break isospin symmetry and use the physical pion masses within the coulomb amplitudes. Actual fits were performed using the TAO package [24].

Results.– The central values and 1σ uncertainties of the πN LECs up to fourth order in χEFT from fitting against scattering data are presented in Table I. For this fit, we find that $\chi_{\text{red}}^2 = 2.29$. As a comparison, the LECs from the fit against WI08 phase shifts of Ref. [9] generate $\chi_{\text{red}}^2 = 3.63$ with respect to our objective function. Not surprisingly, our fit will reproduce experimental data better than the fits with respect to phase shifts. While our LECs are consistent with the spread of previous analyses, we find that no single analysis is entirely consistent with our fit at the 95% confidence level, though the WI08 πN phase shift fit from Ref. [9] lies just outside our interval.

For uncertainty analysis, we apply a standard gradient expansion of $\chi^2(\mathbf{c})$ at the optimum \mathbf{c}_* (see Ref. [25] and references therein for further detail):

$$\chi^2(\mathbf{c}) = \chi^2(\mathbf{c}_*) + \frac{1}{2} \sum_{a,b} (\mathbf{c} - \mathbf{c}_*)_a \mathbf{H}_{a,b} (\mathbf{c} - \mathbf{c}_*)_b + \dots, \quad (4)$$

$$\mathbf{H}_{a,b} = \left. \frac{\partial^2 \chi^2}{\partial c_a \partial c_b} \right|_{\mathbf{c}=\mathbf{c}_*}, \quad (5)$$

where $\chi^2(\mathbf{c})$ is the full (not reduced by n_{df}) objective function. If the residual vectors (R_i and r_j) are normally distributed, then the covariance matrix of our fit is given by

$$\mathbf{C}_{a,b} = \text{cov}(c_a c_b) \approx \chi_{\text{red}}^2 \text{inv}(\mathbf{H})_{a,b}, \quad (6)$$

$$\text{corr}(c_a c_b) = \mathbf{C}_{a,b} / \sqrt{\mathbf{C}_{a,a} \mathbf{C}_{b,b}}. \quad (7)$$

The covariance matrix ($\mathbf{C}_{a,b}$) and correlation matrix $\text{corr}(c_a c_b)$ are presented in table II.

Figure 1 shows calculations of πN scattering observables using our LECs fit data as well as LECs from the phase shift fit of Ref. [9]. At smaller Q_{lab} , the difference is minimal, but it is clear at higher momentum that phase shifts fits are inadequate. This is especially apparent in the calculations of the polarization (P) and spin rotation

TABLE II: Covariance (lower triangle) and correlation (upper triangle) matrices for our fit to experimental data

| LEC | c_1 | c_2 | c_3 | c_4 | $\bar{d}_1 + \bar{d}_2$ | \bar{d}_3 | \bar{d}_5 | $\bar{d}_{14} - \bar{d}_{15}$ | \bar{e}_{14} | \bar{e}_{15} | \bar{e}_{16} | \bar{e}_{17} | \bar{e}_{18} |
|-------------------------------|-------|-------|-------|-------|-------------------------|-------------|-------------|-------------------------------|----------------|----------------|----------------|----------------|----------------|
| c_1 | +0.03 | +0.95 | +0.24 | +0.56 | +0.51 | -0.33 | -0.48 | -0.45 | -0.31 | +0.37 | -0.85 | +0.15 | -0.54 |
| c_2 | +0.07 | +0.21 | -0.08 | +0.55 | +0.54 | -0.37 | -0.48 | -0.56 | -0.32 | +0.56 | -0.96 | +0.18 | -0.54 |
| c_3 | +0.01 | -0.01 | +0.02 | +0.13 | -0.02 | +0.12 | -0.06 | +0.26 | +0.08 | -0.58 | +0.26 | -0.12 | -0.08 |
| c_4 | +0.03 | +0.09 | +0.01 | +0.14 | +0.97 | -0.75 | -0.77 | -0.74 | -0.39 | +0.36 | -0.55 | +0.18 | -0.94 |
| $\bar{d}_1 + \bar{d}_2$ | +0.01 | +0.05 | -0.00 | +0.07 | +0.03 | -0.81 | -0.76 | -0.75 | -0.43 | +0.46 | -0.57 | +0.18 | -0.91 |
| \bar{d}_3 | -0.01 | -0.02 | +0.00 | -0.03 | -0.02 | +0.01 | +0.24 | +0.67 | +0.43 | -0.45 | +0.44 | -0.24 | +0.74 |
| \bar{d}_5 | -0.01 | -0.02 | -0.00 | -0.02 | -0.01 | +0.00 | +0.00 | +0.52 | +0.25 | -0.28 | +0.48 | -0.04 | +0.69 |
| $\bar{d}_{14} - \bar{d}_{15}$ | -0.01 | -0.04 | +0.01 | -0.04 | -0.02 | +0.01 | +0.01 | +0.02 | +0.34 | -0.52 | +0.62 | -0.47 | +0.81 |
| \bar{e}_{14} | -0.02 | -0.05 | +0.00 | -0.05 | -0.03 | +0.02 | +0.01 | +0.02 | +0.13 | -0.80 | +0.50 | -0.28 | +0.41 |
| \bar{e}_{15} | +0.07 | +0.29 | -0.10 | +0.15 | +0.10 | -0.05 | -0.02 | -0.09 | -0.33 | +1.30 | -0.76 | +0.32 | -0.40 |
| \bar{e}_{16} | -0.22 | -0.71 | +0.06 | -0.33 | -0.17 | +0.07 | +0.05 | +0.15 | +0.30 | -1.40 | +2.59 | -0.25 | +0.56 |
| \bar{e}_{17} | +0.01 | +0.05 | -0.01 | +0.04 | +0.02 | -0.02 | -0.00 | -0.04 | -0.06 | +0.22 | -0.24 | +0.36 | -0.50 |
| \bar{e}_{18} | -0.14 | -0.41 | -0.02 | -0.58 | -0.27 | +0.13 | +0.08 | +0.21 | +0.24 | -0.75 | +1.48 | -0.49 | +2.70 |

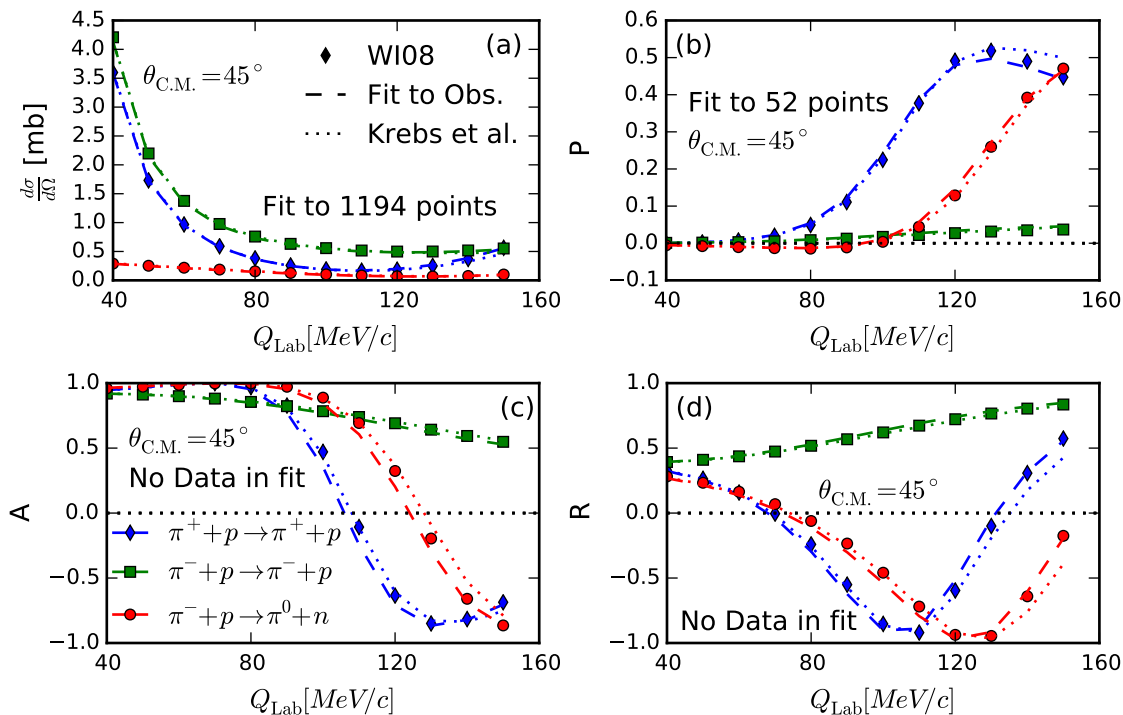


FIG. 1: πN Observables computed at $\theta_{c.m.} = 45^\circ$. The blue (green) lines with diamond (square) markers show results for the $\pi^{+(-)} + p \rightarrow \pi^{+(-)} + p$ processes while the red lines with circular markers show the charge exchange process. The dashed lines show observables computed using our fit to experimental data. The dotted lines shows results reconstructed from LECs of Ref. [9]. P is the polarization, while A and R are the spin rotation parameters, all presented as ratios with respect to the differential cross-section. Definitions of these observables can be found in Ref. [26]

parameters (A and B), suggesting a phase shift fit may not adequately capture the underlying tensor effects that are critical to nuclear observables.

As a validation of our analysis, we plot πN partial wave phase shifts in Fig. 2 and compare with two different partial wave analyses (WI08 [14] and KA84 [12]). The blue bands denotes the 95% CI from our fit. For S- and P-waves, we have good agreement with the WI08 partial wave analysis. In the D-waves, where the $\mathcal{O}(Q^3)$ LECs

have significant contributions, we find poor agreement in the $J = \frac{3}{2}$ channels (D13 and D33).

To better understand where this error in the $J = \frac{3}{2}$ D-waves is coming from, we can use the eigenstate of the covariance matrix to gain insight on the quality of the LEC constraints:

$$C v_j = \nu_j v_j. \quad (8)$$

The vectors of LEC combinations, v_j , form pseudo LECs

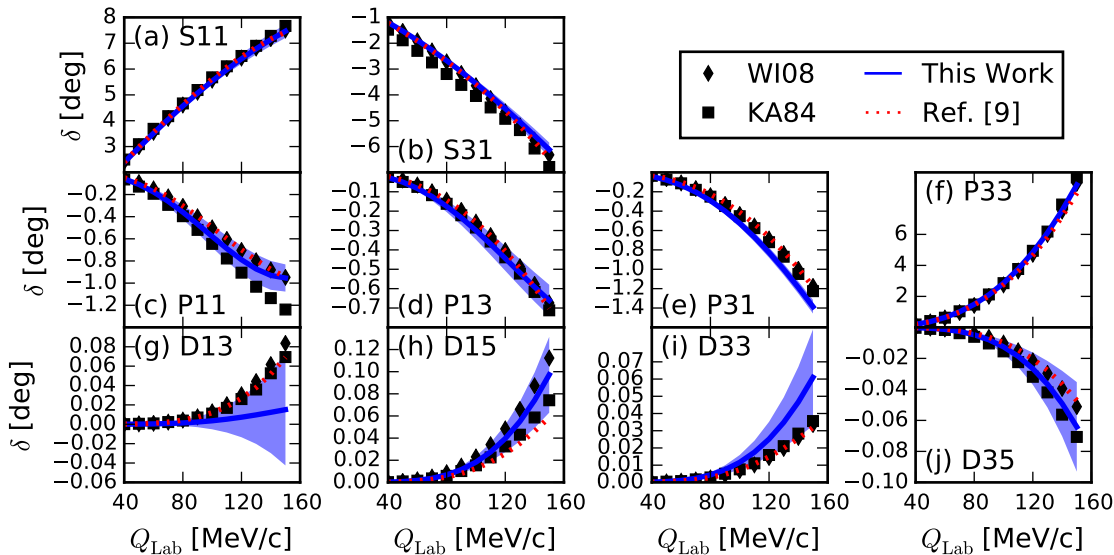


FIG. 2: πN phase shifts. The blue line is a prediction of our fit with the band showing the 95% interval. For comparison, the red dotted lines are the phase shifts from [9]. The markers show phase shifts from two partial wave analyses [12, 14]. The partial waves are denoted as [L][2I][2J] where L is the orbital angular momentum, I is the isospin, and J is the total angular momentum.

that are completely uncorrelated, and eigenvalues ν_j are effective variances of these pseudo LECs. In table III, we examine the LEC content of the least constrained eigenvectors (those with largest eigenvalue). It is clear that the largest eigenvectors are dominated by the \bar{e}_i LECs, and in particular the pair \bar{e}_{16} , \bar{e}_{18} which dominate the two most significant vectors. This indicates that \bar{e}_{16} and \bar{e}_{18} are poorly constrained. Within the scattering amplitudes, \bar{e}_{16} and \bar{e}_{18} span the non-spin-flip and spin-flip amplitudes respectively [9], suggesting that a lack of low momentum data for spin observables could be at fault.

Application to Uncertainty of NN Phase Shifts.— Accurate calculations accompanied with quantitative uncertainty estimates is of-course one of the principal goals of low-energy nuclear theory. This is critical to the study of nuclei near the neutron drip-line or for $0\nu\beta\beta$ decay where this insufficient data to validate many-body calculations.

As a first step towards quantifying the accuracy of the πN sector of the NN interaction, we will predict the confidence intervals of the peripheral ($J \geq 4$) NN scattering phase shifts at $N^3\text{LO}$. These partial waves are fully determined by the long-ranged pion physics. It should also be noted that this is the first $N^3\text{LO}$ calculation of these phase shifts that is actually grounded in experimental scattering data.

Figure 3 shows the predicted 95% CIs of the proton-neutron elastic scattering phase shifts for all total angular momentum $J = 4, 5$ partial waves. For comparison, phase shifts from two different partial wave analyses are presented, PWA93 [10] and SP07 [11]. We also compare to phase shifts computed using the high-precision Idaho- $N^3\text{LO}$ interaction [5], which reproduces the SM99 [27]

TABLE III: Eigenvalues (ν_j) of the covariance matrix, with contributions to eigenvector (v_j) summed over LECs of same chiral order. These eigenvalue correspond to the variances σ_j^2 of effective uncorrelated pseudo LECs. For this analysis the covariance matrix was reduced to a dimensionless form using appropriate powers of the nucleon mass.

| j | ν_j | $\sum_{c_i} v_{j,c_i}^2$ | $\sum_{\bar{d}_i} v_{j,\bar{d}_i}^2$ | $\sum_{\bar{e}_i} v_{j,\bar{e}_i}^2$ | $v_{j,\bar{e}_{16}}^2$ | $v_{j,\bar{e}_{18}}^2$ |
|----|---------|--------------------------|--------------------------------------|--------------------------------------|------------------------|------------------------|
| 1 | 4.1147 | 0.0525 | 0.0094 | 0.9382 | 0.3829 | 0.4207 |
| 2 | 1.4185 | 0.0362 | 0.0052 | 0.9587 | 0.2558 | 0.4798 |
| 3 | 0.5114 | 0.1067 | 0.0013 | 0.8920 | 0.2038 | 0.0038 |
| 4 | 0.2412 | 0.0748 | 0.0236 | 0.9016 | 0.0241 | 0.0157 |
| 5 | 0.0516 | 0.2721 | 0.0459 | 0.6819 | 0.0004 | 0.0021 |
| 6 | 0.0060 | 0.0076 | 0.9696 | 0.0227 | 0.0001 | 0.0044 |
| 7 | 0.0047 | 0.0134 | 0.9647 | 0.0220 | 0.0006 | 0.0008 |
| 8 | 0.0015 | 0.2194 | 0.6919 | 0.0887 | 0.0147 | 0.0368 |
| 9 | 0.0007 | 0.6323 | 0.2427 | 0.1250 | 0.0790 | 0.0002 |
| 10 | 0.0003 | 0.8666 | 0.0346 | 0.0987 | 0.0235 | 0.0348 |
| 11 | 0.0001 | 0.7617 | 0.0125 | 0.2258 | 0.0007 | 0.0007 |
| 12 | 0.0000 | 0.0080 | 0.9918 | 0.0002 | 0.0000 | 0.0000 |
| 13 | 0.0000 | 0.9488 | 0.0068 | 0.0444 | 0.0144 | 0.0001 |

NN database with $\chi_{\text{red}}^2 \sim 1$, and to $N^3\text{LO}$ NN interactions computed using the LECs from Ref. [9]. Our LECs perform quite favorably compared the πN phase shift fit, and surprisingly favorable in many channels to the phase shifts computed from Idaho- $N^3\text{LO}$. For many channels, our error bands are remarkably small.

Conclusions.— We constrained the πN LECs using experimental data with $\chi^2/\text{datum} = 2.29$, generating a set

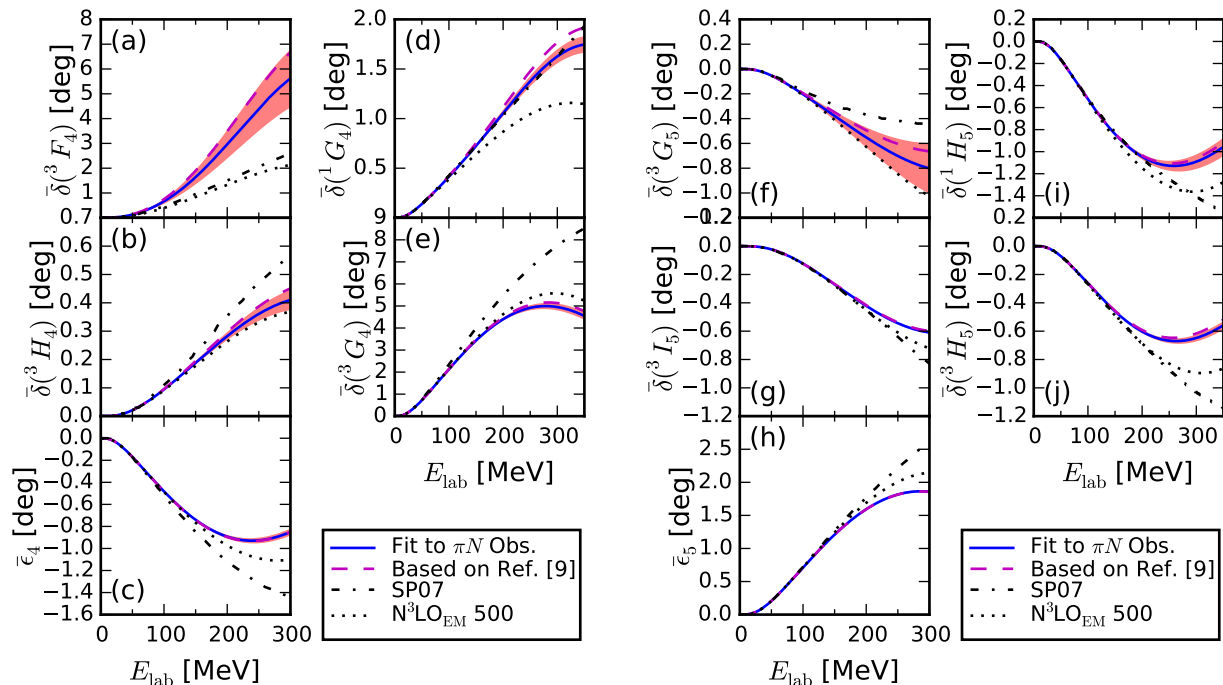


FIG. 3: Elastic proton-neutron $J = 4, 5$ phase shifts at N^3LO ($\Lambda = 500$ MeV) with 95% CIs from πN data (red band). (Dotted line) the phase shifts from the N^3LO interactions of Ref. [28]. (Dashed line) the phase shifts from the Nijmegen partial wave analysis of Ref. [10].

of LECs with error estimates that are compatible for use with modern N^3LO3 Hamiltonians and currents. We find that our lower order LECs are of natural size, while the higher order LECs tend to be unnaturally large (or small in the case of \bar{d}_5 .) We find that even with fairly large error bars for some LECs, the proton-neutron peripheral phase shifts are very well constrained at lab scattering energies below 100 MeV. The πN LECs not only fix the long range part of the N^3LO three body force, but our analysis provides a means to examine uncertainty of the three body force in nuclear bound states as well as uncertainty from currents in observables. Progressing forward, simultaneous constraints of πN and NN LECs with quantitative statistical analysis will yield predictions of few- and

many-body systems with quantified uncertainty and is a topic for many future investigations.

Acknowledgments.— The authors would like to thank H. Krebs, T. Papenbrock, D. Phillips, and R. Workman for their useful discussion. This work was supported in part by the U.S. Department of Energy (DOE) under Grant Nos. DEFG02-96ER40963 (University of Tennessee), de-sc0008499 (NUCLEI SciDAC collaboration), Oak Ridge National Laboratory the Research Council of Norway under contract ISP-Fysikk/216699, and by the European Research Council under the European Community's Seventh Framework Programme (FP7/2007-2013) ERC grant agreement no. 240603. Oak Ridge National Laboratory is supported by the DOE Office of Science under Contract No. DE-AC05-00OR22725.

- [1] P. Maris, J. Vary, and P. Navrátil, *Physical Review C* **87**, 014327 (2013), arXiv:0701038 [nucl-th].
- [2] R. Roth, S. Binder, K. Vobig, A. Calci, J. Langhammer, and P. Navrátil, *Phys. Rev. Lett.* **109**, 052501 (2012).
- [3] H. Hergert, S. K. Bogner, S. Binder, a. Calci, J. Langhammer, R. Roth, and a. Schwenk, *Phys. Rev. C* **87**, 034307 (2013).
- [4] G. Hagen, M. Hjorth-Jensen, G. R. Jansen, R. Machleidt, and T. Papenbrock, *Physical Review Letters* **109**, 032502 (2012), arXiv:arXiv:1204.3612v1.
- [5] D. R. Entem and R. Machleidt, *Phys. Rev. C* **66**, 014002

- (2002).
- [6] A. Ekström, G. Baardsen, C. Forssén, G. Hagen, M. Hjorth-Jensen, G. R. Jansen, R. Machleidt, W. Nazarewicz, T. Papenbrock, J. Sarich, and S. M. Wild, *Physical Review Letters* **110**, 192502 (2013).
- [7] P. Büttiker and U.-g. Meißner, *Nuclear Physics A* **668**, 97 (2000).
- [8] N. Fettes and U.-G. Meißner, *Nuclear Physics A* **676**, 311 (2000).
- [9] H. Krebs, A. Gasparyan, and E. Epelbaum, *Physical Review C* **85**, 054006 (2012).

- [10] V. Stoks, R. Klomp, M. Rentmeester, and J. de Swart, *Phys. Rev. C* **48**, 792 (1993).
- [11] R. Arndt, W. Briscoe, I. Strakovsky, and R. Workman, *Phys. Rev. C* **76**, 025209 (2007).
- [12] R. Koch, *Zeitschrift für Physik C Particles and Fields* **29**, 597 (1985).
- [13] R. Koch, *Nuclear Physics A* **448**, 707 (1986).
- [14] R. L. Workman, R. Arndt, W. J. Briscoe, M. W. Paris, and I. I. Strakovsky, *Physical Review C* **86**, 035202 (2012).
- [15] SAID online program solution WI08, http://gwdac.phys.gwu.edu/analysis/pin_analysis.html.
- [16] See Refs. [11] for details on their process for a slightly older solution (SP06).
- [17] N. Fettes, U.-G. Meißner, and S. Steininger, *Nuclear Physics A* **640**, 199 (1998).
- [18] N. Fettes, *Ann. Phys.* **283**, 273 (2000).
- [19] N. Fettes and U.-G. Meißner, *Nuclear Physics A* **693**, 693 (2001).
- [20] B. Tromborg, S. Waldenstrøm, and I. Øverbø, *Helvetica Physica Acta* **51** (1978), 10.5169/seals-114961.
- [21] B. Tromborg and J. Hamilton, *Nuclear Physics B* **76**, 483 (1974).
- [22] B. Tromborg, S. Waldenstrøm, and I. Øverbø, *Physical Review D* **15**, 725 (1977).
- [23] D. Bugg, *Nuclear Physics B* **58**, 397 (1973).
- [24] T. Munson, J. Sarich, S. Wild, S. Benson, and L. C. McInnes, *TAO 2.0 Users Manual*, Tech. Rep. ANL/MCS-TM-322 (Mathematics and Computer Science Division, Argonne National Laboratory, 2012) <http://www.mcs.anl.gov/tao>.
- [25] J. Dobaczewski, W. Nazarewicz, and P.-G. Reinhard, *Journal of Physics G: Nuclear and Particle Physics* **41**, 074001 (2014), arXiv:1402.4657.
- [26] G. Höhler, *Pion Nucleon Scattering. Part 2: Methods and Results of Phenomenological Analyses*, edited by H. Schopper, Landolt-Börnstein - Group I Elementary Particles, Nuclei and Atoms, Vol. 9b2 (Springer Berlin Heidelberg, Berlin, Heidelberg, 1983).
- [27] R. Machleidt, *Phys. Rev. C* **63**, 024001 (2001).
- [28] D. R. Entem and R. Machleidt, *Phys. Rev. C* **68** (2003), 10.1103/PhysRevC.68.041001.